JOURNAL OF GEOPHYSICAL RESEARCH, VOL. 105, NO. C8, PAGES 19,729–19,737, AUGUST 15, 2000

Propagation of swell across a wide continental shelf

T. H. C. Herbers and E. J. Hendrickson

Department of Oceanography, Naval Postgraduate School, Monterey, California

W. C. O'Reilly

Center for Coastal Studies, Scripps Institution of Oceanography, La Jolla, California

Abstract. The transformation of ocean swell across a wide, shallow (nominal depths 25–50 m) continental shelf is examined with data from a 100 km long transect of bottom pressure recorders extending from the shelf break to the beach at Duck, North Carolina. The analysis is restricted to periods with light winds when surface boundary layer processes (e.g., wave generation by wind and wave breaking in the form of whitecaps) are expected to be relatively unimportant. The majority of the observations with low-energy incident swell conditions (significant wave heights <1 m) shows weak variations in swell energy across the shelf, in qualitative agreement with predictions of a spectral refraction model. Although the predicted ray trajectories of waves propagating over the irregular shelf bathymetry are quite sensitive to the deep water incident wave directions, the predicted spatial energy variations for broadbanded wave fields are small and relatively insensitive to incident wave conditions, consistent with the observations. Whereas swell dissipation on the shelf appears to be insignificant in low-energy conditions, strong attenuation of swell energy levels (a factor 4 between the shelf break and nearshore sites) was observed in high-energy conditions (significant wave height 2.5 m). This decay, not predicted by the energy-conserving refraction model, indicates that dissipative bottom boundary layer processes can play an important role in the transformation of swell across wide continental shelves.

1. Introduction

In many coastal regions the transformation of swell from the open ocean to the beach is strongly affected by propagation over the continental shelf. Refraction of waves propagating over shoals, ridges, canyons, and other shelf features can cause dramatic spatial variations in wave heights [e.g., *Munk and Traylor*, 1947]. Refraction effects on the evolution of wave spectra can be evaluated for arbitrary two-dimensional continental shelf topography by applying an energy balance along ray trajectories [e.g., *Munk and Arthur*, 1951; *Longuet-Higgins*, 1957; *Le Méhauté and Wang*, 1982]. This numerically accurate Lagrangian (i.e., following wave groups) method predicts the gross variations in wave energy observed along the bathymetrically complex southern California coast [*O'Reilly et al.*, 1994]. Significant refraction effects are predicted not only when waves pass over a single large submarine obstacle but also when waves travel through a large shallow coastal region with benign topography [e.g., *Graber et al.*, 1990; *O'Reilly and Guza*, 1993].

In refraction theory, wave amplitude variations are assumed to be small over scales comparable to the surface wavelength. This assumption is typically violated in the vicinity of large topographic shelf features or if the wave spectrum is extremely narrow. In these situations, models based on the mild slope equation [*Berkhoff*, 1972] that incorporate both refraction and diffraction effects are more accurate, as has been demonstrated with laboratory measurements of waves propagating over an elliptical shoal [e.g., *Panchang et al.*, 1990]. Mild slope equation models have been extended to include wave reflection from subwavelength scale depth variations [*Kirby*, 1986a] and abrupt bathymetry features [*Porter and Staziker*, 1995], but these numerically expensive models have not been applied yet to large continental shelf regions. The more widely used parabolic approximations of the mild slope equation [e.g., *Radder*, 1979; *Kirby*, 1986b, c] are well suited to combined refraction-diffraction computations over large domains but may be inaccurate in situations where refraction causes large changes in wave direction. Although the limitations of refraction and combined refraction-diffraction models are not yet fully understood, intercomparisons of the predicted evolution of realistic wave spectra over benign shelf bathymetry show generally good agreement [*O'Reilly and Guza*, 1991, 1993].

Swell can traverse entire ocean basins with very little loss in energy [*Snodgrass et al.*, 1966]. However, significant dissipation is believed to take place in the bottom boundary layer of a shallow continental shelf. *Shemdin et al.* [1980] suggested that a variety of bottom processes, including bottom friction, percolation through the bottom, and wave-induced bottom motion, may cause significant damping of swell propagating across a wide continental shelf, but the damping rates appear to be strongly dependent on the sediment type, bottom microtopography, and local currents; all of which are often unknown. Laboratory and field measurements show that bottom friction is particularly sensitive to the presence of ripples that are usually formed in low-energy wave conditions by the near-bed oscillatory wave motion and subsequently obliterated by stronger flows in high-energy wave conditions [e.g., *Grant and Madsen*, 1986, and references therein). These transient, small-scale bed forms are extremely difficult to quantify on a natural seabed.

Paper number 2000JC900085.
0148-0227/00/2000JC900085$09.00

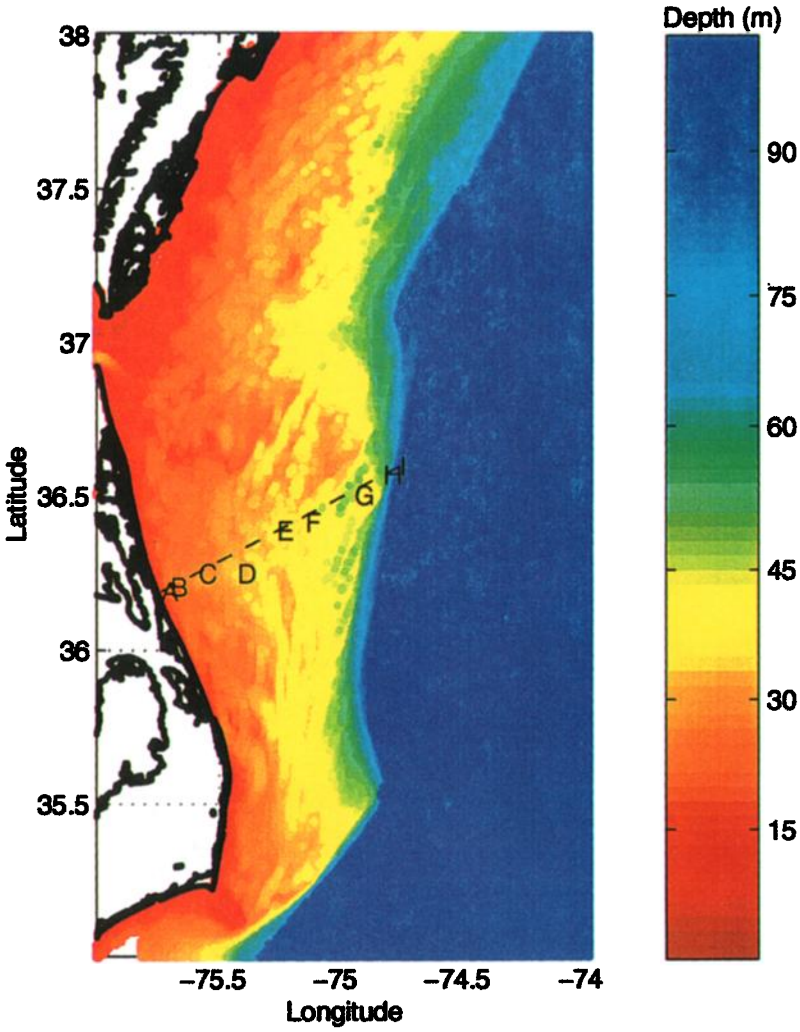

Plate 1. Plan view of the bathymetry of the North Carolina shelf in the numerical model domain. The instrumented transect is indicated with a dashed line, with letters denoting the pressure sensor sites (site D is 7.5 km south of the transect).

Very few measurements of the attenuation of swell in shallow water have been reported. *Hasselmann et al.* [1973] examined the swell decay observed during the Joint North Sea Wave Project (JONSWAP) experiment with a 160 km long cross-shore transect of various types of instruments deployed off the coast of Germany. The observed damping rates did not agree with generally accepted formulations of bottom friction and suggested that other attenuation mechanisms such as backscattering of swell from small-scale bottom irregularities may be important [*Long*, 1973]. *Young and Gorman* [1995] reported 2 week long observations from a similar transect of instruments spanning the continental shelf on the southern coast of Australia and used these measurements in conjunction with the third-generation wave prediction model WAM [*The WAMDI Group*, 1988] to estimate the contribution of bottom friction to the observed overall decrease in swell energy across the shelf. The results suggest that the strong attenuation of energetic southern ocean swells observed at shallow instrument sites is caused primarily by bottom friction with estimated drag coefficients that are much larger than the values commonly used in wave prediction models.

New observations of the transformation of swell across a continental shelf are presented here. A 100 km long cross-shelf transect of 10 bottom pressure recorders was deployed off the coast of North Carolina. The field experiment and data analysis (restricted to periods of light winds when swell transformation across the shelf is expected to be dominated by bottom processes) are described in section 2. A spectral refraction model, based on a backward ray-tracing scheme [*O'Reilly and Guza*, 1993] was applied to a fine-resolution (200 m) bathymetry grid. The effects of the undulating shelf topography on the transformation of swell are illustrated with model simulations in section 3. Observed variations in swell energy across the shelf are compared to model predictions initialized with data from a directional buoy located near the seaward end of the transect in section 4. Discrepancies between measured swell energy levels and the energy-conserving model predictions are used to quantify crudely bottom damping effects in section 5, and a summary is given in section 6.

2. Experiment and Data Analysis

The field data used in this study were collected as part of the Duck94 Nearshore Processes Experiment conducted offshore

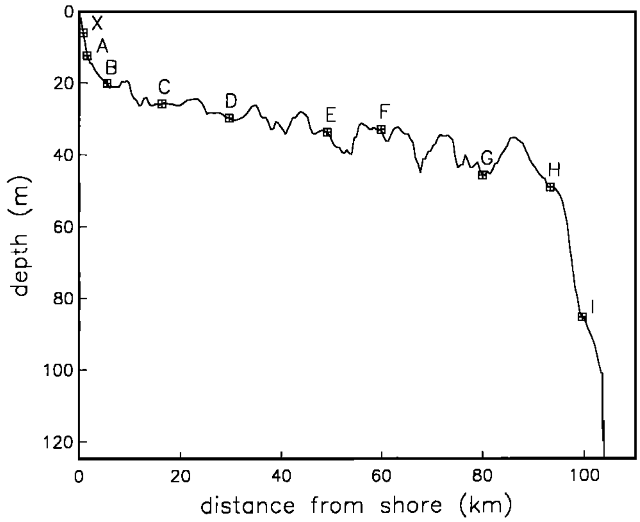

Figure 1. Cross section of the instrumented transect of the North Carolina shelf (dashed line in Plate 1).

of the U.S. Army Corps of Engineers Field Research Facility (FRF) near Duck, North Carolina, between late July and early December 1994. The coast consists of a series of relatively straight barrier islands with sandy beaches that are exposed to the Atlantic Ocean. The continental shelf is 50–100 km wide and only 20–50 m deep (Plate 1). Ten battery-powered internally recording bottom pressure sensors were deployed along a cross-shelf transect extending from the Duck beach to the shelf break (Plate 1, the stations are represented by letters). The shallowest instrument X was mounted on a pipe jetted into the beach 6 m deep just outside the surf zone. At all other sites (depths ranging from 12 to 87 m, Figure 1) the instruments were mounted inside the anchor of a surface mooring. Each of the autonomous instrument packages contained a Setra capacitance-type pressure transducer, a Tattletale microprocessor, and a disk drive for data storage. Pressure data were recorded nearly continuously with a 2 Hz sample rate during the 4 month long deployment. Some malfunctioning data acquisition systems were replaced with a cassette tape data storage system utilizing a reduced sampling scheme (one 137 min long record sampled at 1 Hz every 3 hours). Site B suffered significant data loss during the first 2 months of the experiment, and the two shallowest instruments (X and A) failed during Hurricane Gordon on November 18. The shallowest site X (6 m depth) and the deepest site I (87 m depth) are excluded from the present analysis because the beach was not adequately resolved in the numerical refraction calculations and high-frequency ($\geq$0.1 Hz) swell was strongly attenuated over the water column in 87 m depth. Measurements of directional properties of the incident swell were available from a National Data Buoy Center (NDBC) 3 m discus buoy located within 2 km of site H.

Surface elevation spectra were computed from 12 hour long bottom pressure records using a linear theory depth correction. Relatively long data records were used in the analysis because the travel time of swell traversing the shelf is of the order of a few hours. Nonstationary conditions (i.e., temporal variations in spectral levels of more than 30% over a 12 hour run) were excluded from the analysis because the model predictions do not account for time lags in swell arrivals at different sites. The analysis was restricted to longer period (0.05–0.10 Hz) waves, which are usually remotely generated and feel the bottom on the entire shelf. Periods of moderate to strong local winds (speeds $>$10 m s^{-1}) with possibly significant generation effects on the shelf at wave frequencies $<$0.10 Hz were excluded from the analysis. During the periods of light winds considered in this study, currents on the shelf were predominantly tidal with speeds generally $<$0.5 m s^{-1} [*Haus et al.*, 1995]. Long-period swells are not significantly affected by these weak currents. The analysis was restricted further to cases with mean swell propagation directions (measured near site H) within $\pm$35° of normal incidence (100°) to the shelf break. Observations with larger northerly or southerly swell incidence angles were excluded because waves approaching the shelf at large oblique angles are strongly refracted over the continental slope seaward of the instrumented transect, and thus the deep water directional properties of these waves are not well represented by the NDBC buoy measurements collected at the shelf break (in 48 m depth near site H). On the basis of these considerations the original data set of 244 observations was reduced to 71 observations with significant wave heights ranging from 0.1 to 2.5 m.

The variability of swell energy levels on the shelf is summarized in Figure 2 with the observed total swell variances at four sites spanning the shelf. Energy variations across the shelf were generally small ($<$30%), with the exception of the single most energetic event (Julian days 290–295) when a large (up to 70%) decrease in energy was observed between the deepest and shallowest sites.

Accurate predictions of swell refraction require detailed shelf bathymetry. A high-resolution digital bathymetry database was available from the National Ocean Service (NOS), National Geophysical Data Center (NGDC). Unfortunately, this database contains large gaps extending from 36.2° to 36.8°N and from the coast to 74.8°W. To fill these gaps, additional bathymetric surveys were conducted during instrument deployment and recovery cruises with a precision depth recorder mounted on the hull of the R/V *Cape Hatteras*. The survey tracks were spaced at ~1 km intervals. The Fathometer measurements were detided using sea level data from a tide gauge located near site A on the FRF pier. Cross-shelf differences between the tidal fluctuations measured with the 10 bottom pressure sensors (Figure 1) are negligibly small ($<$10 cm). Other bathymetry errors that are difficult to quantify include navigational inaccuracies of vessels used in the older surveys and the accretion and erosion of the sandy bottom in shallow regions.

Data from the combined surveys were used to create a fine-resolution ($\approx$200 m) bathymetry grid for the area 35° to 38°N and 74° to 76°W using the Delaunay tessellation interpolation method of *Watson* [1982]. The grid distortion resulting from the transformation to Cartesian coordinates is small (maximum wave propagation direction errors of about 1° [*O'Reilly and Guza*, 1993]).

3. Spectral Refraction Computations

The North Carolina continental shelf is characterized by a wide midshelf region with shore oblique ridges (Plate 1). Low-frequency swell may be strongly refracted by these large (O(10 km) wide) features with heights up to 10 m (Figure 1). To quantify the importance of the irregular shelf topography to the spatial variability of swell energy, spectral refraction com-

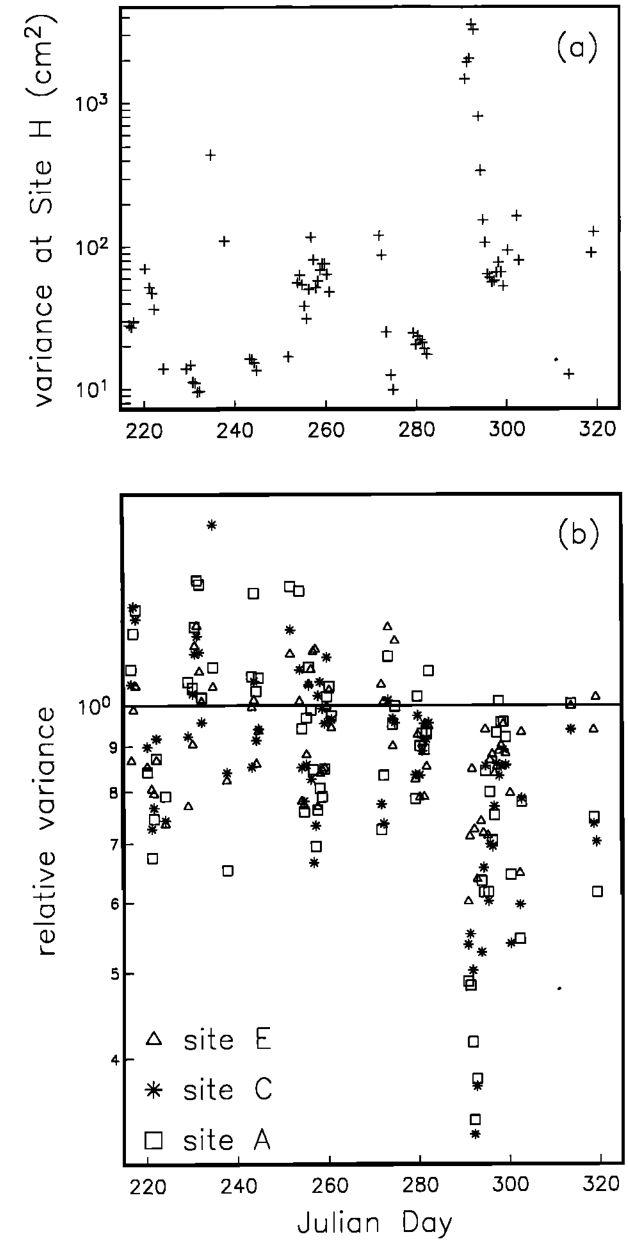

Figure 2. Observed swell variability on the shelf for the 71 data runs analyzed in this study: (a) swell variance at the outer shelf site H and (b) swell variances at sites E (midshelf), C (inner shelf), and A (nearshore) normalized by the variance at site H.

putations were carried out for a range of deep water incident wave conditions. The incident wave field is assumed to be stationary and spatially homogeneous in the surrounding deep Atlantic waters and described by a frequency directional spectrum $E_0(f, \theta_0)$ (subscripts $_0$ indicate deep water values). Wave generation on the shelf, nonlinear interactions, and dissipation are neglected. For a given deep water spectrum $E_0(f, \theta_0)$, predictions of the transformed spectrum $E(f, \theta)$ at eight of the instrumented sites A–H (Plate 1) were obtained with a backward ray-tracing technique [*O'Reilly and Guza*, 1991].

From each site, rays were traced in all possible directions back to deep water using the ray equations [*Munk and Arthur*, 1951; *Le Méhauté and Wang*, 1982]:

$$\frac{dx}{ds} = \cos\theta, \tag{1a}$$

$$\frac{dy}{ds} = \sin\theta, \tag{1b}$$

$$\frac{d\theta}{ds} = \frac{1}{c}\left(\sin\theta\,\frac{\partial c}{\partial x} - \cos\theta\,\frac{\partial c}{\partial y}\right), \tag{1c}$$

where c is the phase speed, θ is the propagation direction, s is the distance measured along a ray, and (x, y) are the horizontal space coordinates. Equations (1a)–(1c) were integrated using a fourth-order Runge-Kutta method. Initially, rays were computed for all possible shallow water angles θ at 1° increments and terminated upon reaching deep water, land, or the boundaries of the grid. These angles were subsequently bisected with additional rays until the spacing of the resulting deep water angles θ_0 of adjacent rays was everywhere <2.5° (see *O'Reilly and Guza* [1991] for further details). The complete set of ray trajectories for a given shallow water site yields an estimate of an inverse direction function Γ:

$$\theta_0 = \Gamma(f, \theta), \tag{2}$$

which defines the relationship between the deep water incidence angle θ_0 and the refracted propagation direction θ at a shallow water site.

Examples of the inverse direction function Γ for representative swell frequencies f = 0.10 and 0.07 Hz are shown in Figure 3. On the outer shelf at site H (49 m depth), 0.10 Hz waves are not yet significantly refracted, and $\theta_0 \approx \theta$ (Figure 3a). Longer wavelength 0.07 Hz waves are affected by propagation over the continental slope seaward of site H, resulting in transformed wave directions at site H that are slightly refracted toward normal incidence to the shelf break (≈100°) (Figure 3b). The Γ functions predicted at site H are smooth because the seabed seaward of site H is smooth with approximately straight and parallel depth contours.

The more complicated inverse direction functions predicted at the inner shelf site C (25 m depth, Figures 3c and 3d) show the strong cumulative effect of wave refraction over the irregular shelf bathymetry. The direction changes are small (<10°) for 0.1 Hz waves arriving at the shelf break with angles θ_0 that are within ±20° of normal incidence ($\theta_0 \approx$ 100°). Large differences between θ_0 and θ (up to 70°) are predicted for θ_0 < 80° and θ_0 > 120°. Waves arriving from southerly angles (θ_0 > 150°) are strongly refracted by the curvature of the coast and a group of shoals near Cape Hatteras (35.2°N, 75.5°W, Plate 1). Although the bathymetry is smoother to the north of the instrumented transect, the shelf is considerably wider and curves to the east (Plate 1), resulting in longer propagation distances over the shelf for waves arriving from northerly angles (θ_0 < 60°) and comparably strong refraction effects. Pronounced refraction effects on the shelf are predicted for lower-frequency 0.07 Hz waves arriving from deep water at all angles (Figure 3d).

Large (20°–70°) variations in θ_0 predicted for small (1°) changes in θ at site C (Figures 3c and 3d) indicate a strong sensitivity of ray trajectories to the irregular shelf topography. Additionally, many gaps in the Γ function (i.e., ray trajectories with turning points that do not extend to the open ocean) of 0.07 Hz waves suggest that wave trapping on the continental shelf may occur at swell frequencies even for waves propagating in directions nearly normal to the coastline.

The refraction transformation of the frequency-directional

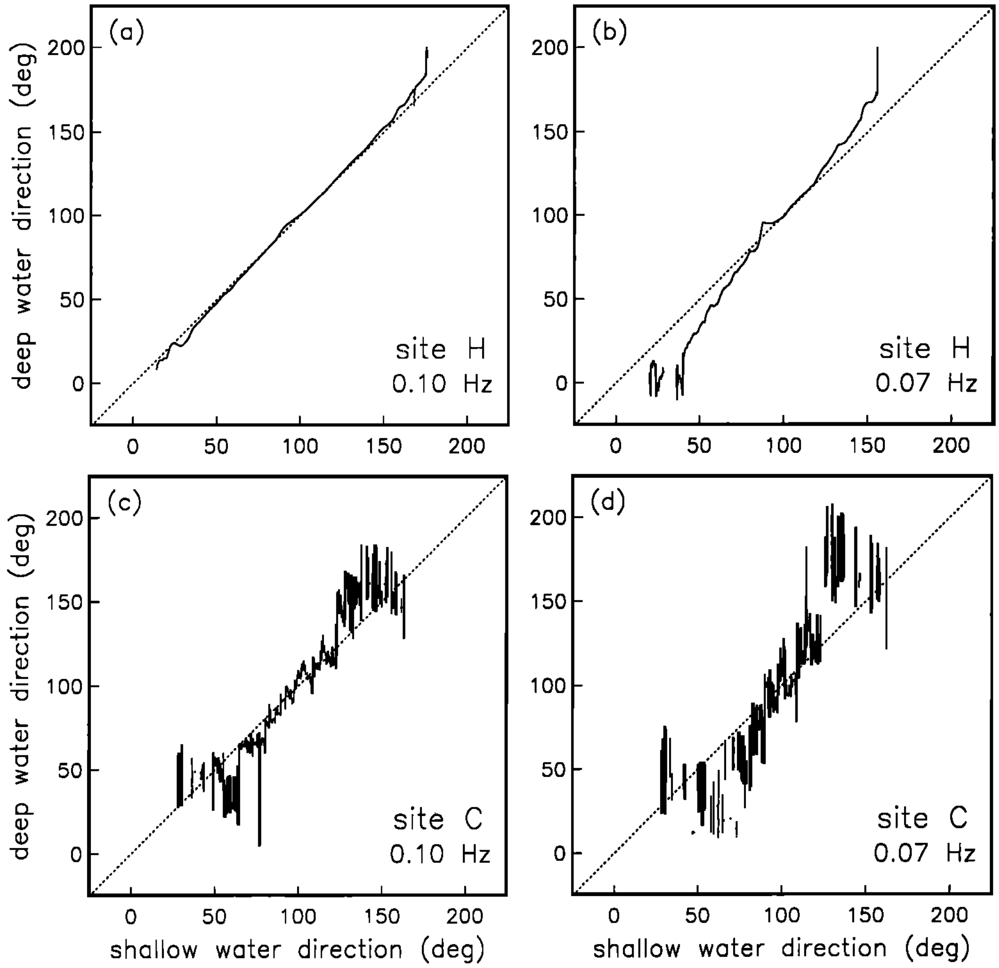

Figure 3. Predictions of the inverse direction function Γ (equation (2)) for waves with frequencies (left) 0.10 Hz and (right) 0.07 Hz arriving at (top) the outer shelf site H and (bottom) the inner shelf site C.

wave spectrum from deep ($E_0(f, \theta_0)$) to shallow ($E(f, \theta)$) water is given by

$$E(f, \theta) = \frac{c_0}{c}\frac{c_{g0}}{c_g} E_0[f, \Gamma(f, \theta)], \qquad (3)$$

where c_g is the group velocity [*Longuet-Higgins*, 1957; *Le Méhauté and Wang*, 1982]. Numerical simulations of the refraction transformation of swell arriving from a single remote source were carried out with a simple cosine power directional distribution of wave energy in deep water:

$$E_0(\theta_0) \propto \cos^{2m}\left(\frac{\theta_0 - \theta_{\mathrm{mean}}}{2}\right). \qquad (4)$$

The mean propagation direction θ_{mean} was varied in the simulations from 50° to 150° with values of the directional spreading parameter $m = 100$, 50, and 25 (i.e., full beam widths at half maximum power of 20°–40°). The wave energy was distributed uniformly over a 0.01 Hz wide frequency band centered at a representative ocean swell frequency (0.07 and 0.1 Hz).

The cross-shelf variability of wave energy is illustrated in Figure 4 with predictions of transformed wave energy at sites H (outer shelf, 49 m depth), E (midshelf, 35 m), C (inner shelf, 25 m), and A (near the shore, 12 m) for incident waves with a deep water directional spread $m = 50$. The predicted wave energies (integrated over all directions and normalized by the deep water incident wave energy) are shown as a function of the mean incidence angle θ_{mean} in deep water. For 0.1 Hz waves (Figure 4a) the cross-shelf energy variations are <20% for a wide range of mean wave directions, but a significant decrease (up to ~50%) in energy is predicted at the shallower sites C and A for southeasterly deep water incidence angles ($\theta_{\mathrm{mean}} = 120$–150°). Larger cross-shelf variations in wave energy are predicted for the 0.07 Hz swell. For θ_{mean} close to normal incidence (100°), energy levels are ~40% smaller at midshelf site E and 30% larger at nearshore site A (compared to the deep water levels). Although propagation effects are also significant on the outer shelf, small changes in energy are predicted between deep water and site H owing to the canceling effects of shoaling (a 20% reduction in energy resulting from an increase in group speed) and focusing (note in Figure 3b that angles θ in the range 85°–95° transform to the same deep water angle $\theta_0 \approx 95°$). Whereas at sites H, C, and A the predicted energy levels generally decrease with increasing oblique incidence angle, qualitatively similar to wave energy transformation over an alongshore uniform shelf, the response at site E is maximum for oblique northerly (70°) and southerly (130°) angles. These differences illustrate the important focusing effects of the two-dimensional shelf topography.

Although the predicted ray trajectories are very sensitive to

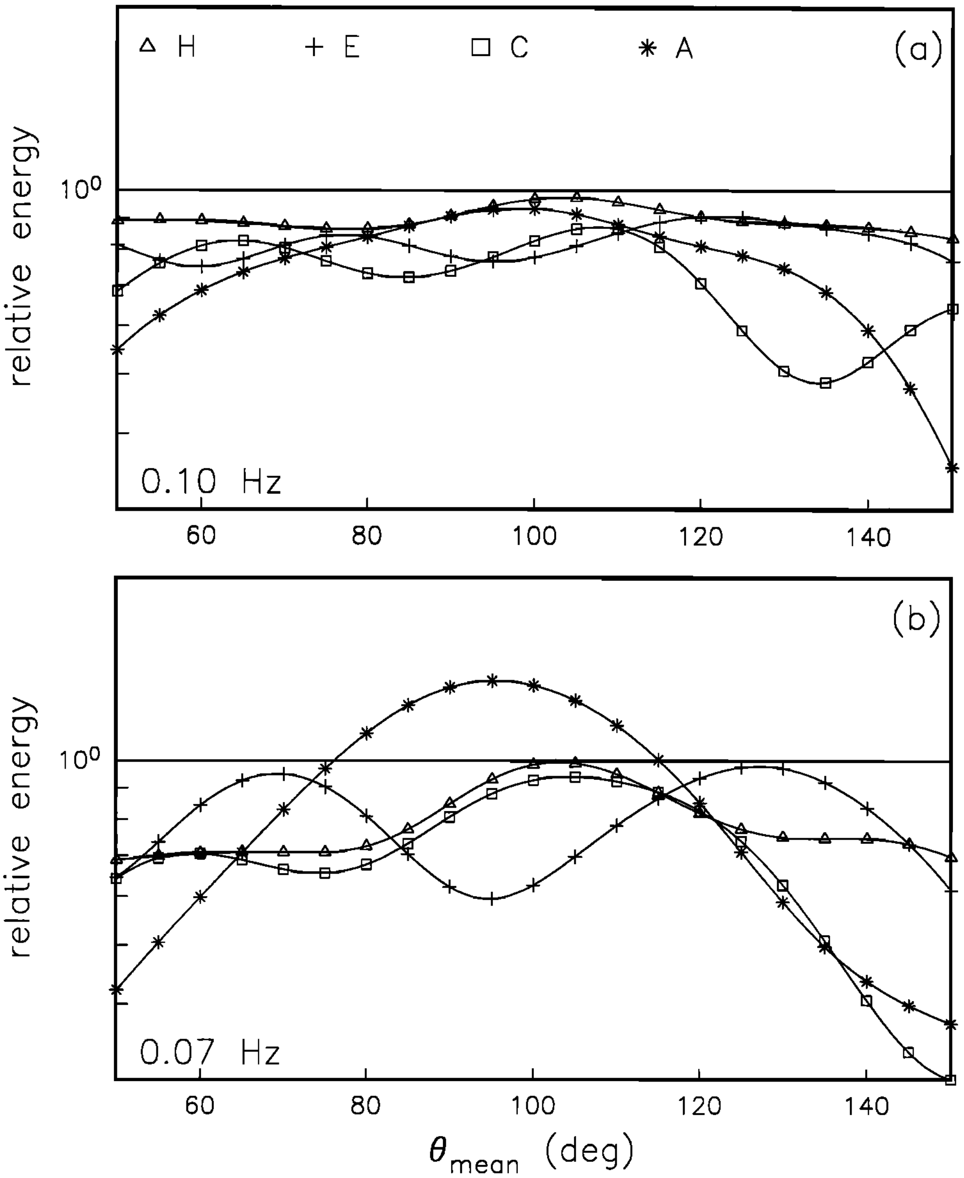

Figure 4. Predicted energy relative to deep water at sites H, E, C, and A for waves with a mean frequency of (a) 0.10 and (b) 0.07 Hz as a function of the mean incidence angle in deep water. The incident wave energy is distributed uniformly over a 0.01 Hz wide band with a narrow cosine power directional distribution (m = 50).

the detailed shelf topography (Figure 3), the predicted swell energy levels are generally within a factor of 2 of the deep water value and do not show a strong sensitivity to the mean incident wave direction (Figure 4). Small differences (<20%) in energy levels predicted at inner shelf sites for different values of the directional spreading parameter m (25 and 100, not shown) indicate that the transformation of swell across the shelf is also relatively insensitive to the width of the directional spectrum. For realistic spectral widths the strong topographic effects on individual components of the incident wave spectrum appear to cancel, yielding smooth spatial variations in wave energy and a weak dependence of the energy transformation on the directional properties of incident waves.

4. Model-Data Comparisons

Swell spectra estimated from 12 hour long data records at each instrument site (section 2) are compared here to predictions of an energy-conserving spectral refraction model (section 3) initialized with directional wave measurements near the shelf break. Directional distributions of incident swell energy in 0.01 Hz wide frequency bands (centered at 0.05, 0.06, 0.07, 0.08, 0.09, and 0.10 Hz) were estimated from the NDBC buoy measurements using the maximum entropy method [*Lygre and Krogstad*, 1986]. These estimates do not resolve the detailed structure of the directional wave spectrum, but refraction model simulations for realistic wave spectra do not indicate a strong sensitivity to the directional properties of incident waves (e.g., Figure 4).

Comparisons of predicted and observed swell variances for all 71 data records are summarized in Figure 5. Ratios between observed and predicted swell variances are shown versus the deep water swell variance for midshelf site E, inner shelf site C, and nearshore site A. For most data sets the predicted variances at all sites (including those not shown in Figure 5) are within ±40% of the observed variances. In benign conditions with offshore swell variances ≤60 cm^2 (i.e., significant wave heights $H_s < 0.3$ m) the predicted swell energy levels at the shallower sites are consistently lower (by as much as a factor 2) than the observed levels (Figures 5b and 5c). Similar discrepancies were reported by *Young and Gorman* [1995] and attributed to spatial variations in deep water incident wave conditions in the absence of a well-defined swell system.

In the relatively few high-energy swell cases with deep water variances $>10^3$ cm^2 ($H_s > 1.3$ m) the energy levels observed at the shallower sites are much lower than the predicted levels, indicating strong attenuation of swell on the shelf that is not accounted for in the energy-conserving model predictions. Although the largest discrepancies between model predictions and observations occur with low-frequency swells that are affected most severely by the shelf topography (Figure 4), the discrepancies are small for low-energy cases with comparably low peak frequencies (Figure 5, squares). The strong energy dependence of the observed swell decay is inconsistent with linear wave-bottom interaction processes (e.g., backscattering, percolation, and wave-induced bottom motion; discussed by *Shemdin et al.* [1980]) and suggests that swell energy is dissipated on the shelf.

The strongest swell decay was observed on October 19 when the incident wave energy was maximum ($H_s \approx 2.5$ m). The observed and predicted cross-shore evolution of swell energy levels is shown in Figure 6. The wave field is characterized by long-period (peak frequency 0.07 Hz) swell that arrived at the shelf break from 83° (i.e., close to normal incidence) and propagated almost straight down the instrumented transect (Plate 1). The observed local wind speed was <5 m s^{-1}, indicating that wave generation and surface dissipation processes were negligible. Weak refraction effects result in predicted energy levels that are within ±20% of the deep water energy at all instrumented sites (Figure 6). Observed energy levels show a gradual monotonic decrease from the shelf break to the shoreline. At the shallowest instrument (1 km from shore) the observed swell variance is only ~25% of the predicted value. The observed strong attenuation of swell energy levels in the absence of local winds suggests a gradual loss of energy in the bottom boundary layer. Simultaneous airborne remote sensing measurements using a scanning radar altimeter [*Hwang et al.*, 1998] show a swell decay across the shelf that is qualitatively similar to the in situ observations presented here.

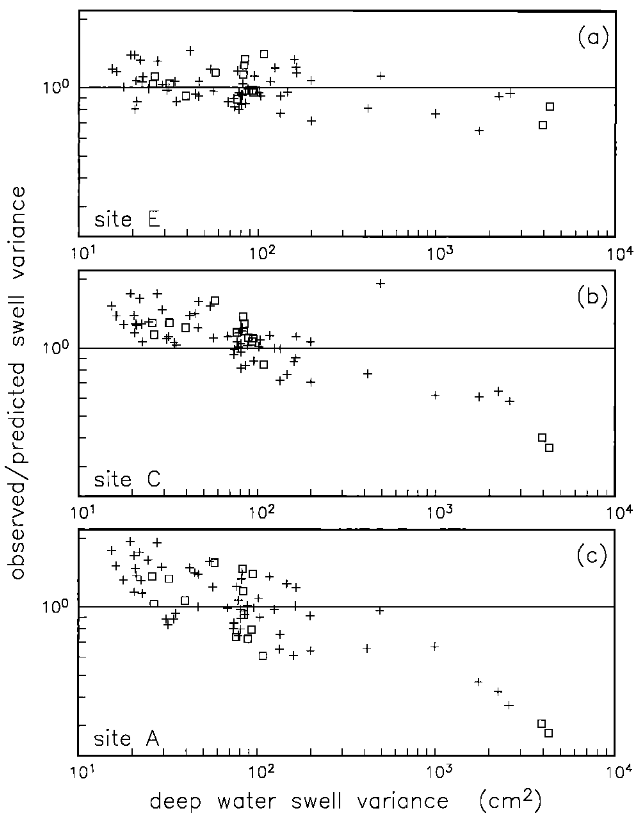

Figure 5. Ratio of observed and predicted swell variances at (a) midshelf site E, (b) inner shelf site C, and (c) nearshore site A versus deep water swell variance. Different symbols are used to differentiate wave fields with peak frequencies below 0.075 Hz (squares, 15 cases) and above 0.075 Hz (asterisks, 56 cases).

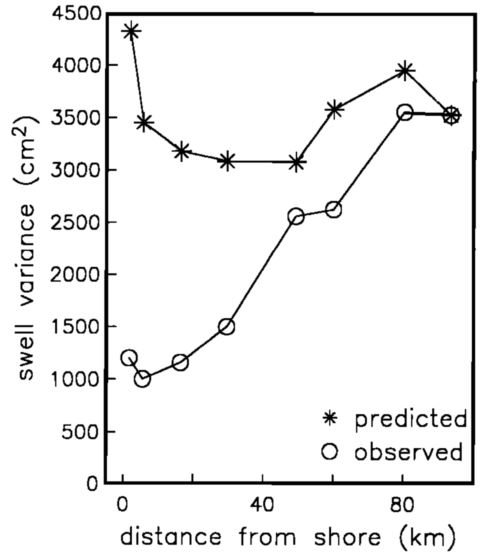

Figure 6. Predicted and observed swell variance versus distance from shore, on October 19, 1994, when the deep water swell variance was maximum.

Frequency spectra observed at three sites spanning the shelf are compared with predicted spectra in Figure 7. At midshelf site E the observed and predicted spectra are in good agreement at frequencies ≥0.08 Hz, whereas observed levels at the spectral peak are ~40% lower than the predicted levels. On the outer shelf, energy is apparently lost only by lower-frequency components of the spectrum, possibly because high-frequency components with relatively short wavelengths are attenuated at the bottom. At the shallower sites C (inner shelf) and A (nearshore), observed spectral levels are lower than predicted spectral levels at all frequencies, suggesting significant damping of all components of the spectrum. The apparent damping is strongest near the peak frequency, causing a slight broadening of the observed spectrum at site A.

5. Discussion

The observed strong decay of energetic swell across the continental shelf in light wind conditions suggests that large energy losses can occur in the bottom boundary layer. A bottom dissipation mechanism that is believed to be important for long waves propagating over a shallow sandy bottom is the turbulent friction in the bottom boundary layer associated with

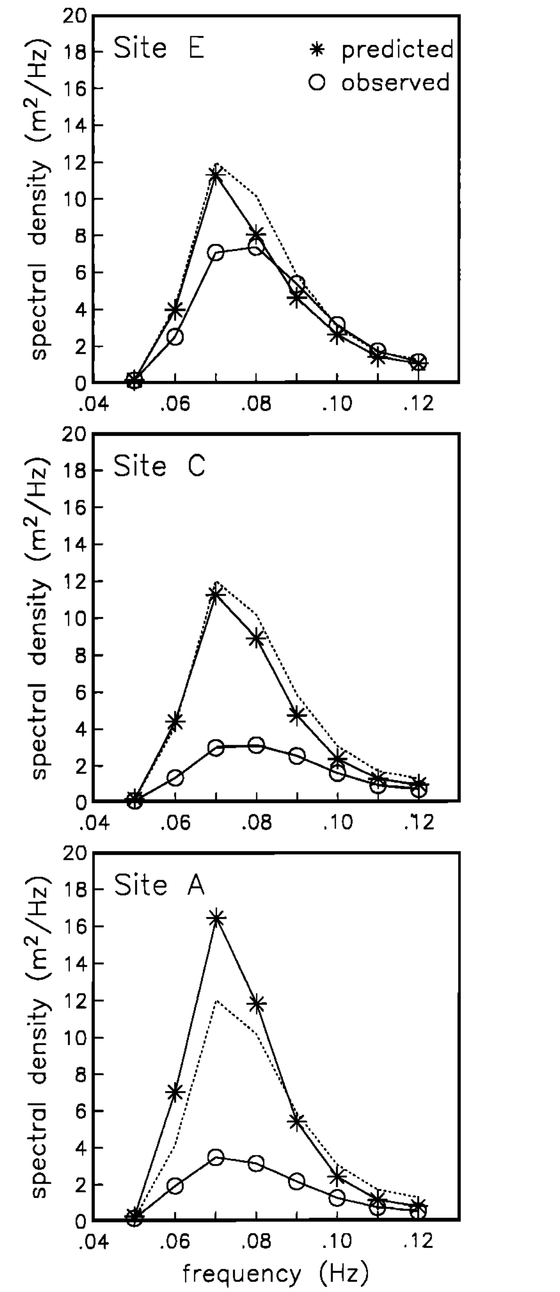

Figure 7. Predicted and observed swell spectra at (a) midshelf site E, (b) inner shelf site C, and (c) nearshore site A on October 19, 1994, when the deep water swell variance was maximum. The incident swell spectrum observed at the outer shelf site H is indicated with a dotted curve.

the oscillatory wave motion. The effects of bottom friction are often modeled using a simple quadratic friction law,

$$\boldsymbol{\tau} = \tfrac{1}{2}\rho f_w \mathbf{u}_b |\mathbf{u}_b|, \tag{5}$$

where $\boldsymbol{\tau}$ is the instantaneous bottom shear stress, $\mathbf{u}_b$ is the instantaneous horizontal velocity vector of the orbital wave motion just above the bottom boundary layer, and f_w is a friction factor that depends on the roughness of the seabed. A crude estimate of a friction factor f_w required to explain the cross-shelf decay observed in Figure 6 is obtained from the simple analytic expression for the damping of a monochromatic wave train in uniform water depth [*Putnam and Johnson*, 1949; see also *Tolman*, 1992]:

$$\frac{dE}{dx} = -f_w \frac{32\sqrt{2}\,\pi^2 f^3}{3gc_g \sinh^3(kh)} E^{3/2}. \tag{6}$$

Substitution of a representative shelf depth (h = 35 m), the spectral peak frequency ($f = 0.07$ Hz) with the corresponding linear wavenumber and group speed, an average (midshelf) observed wave variance ($E \approx 0.23$ m^2), and an average observed attenuation rate ($dE/dx \approx 3.5 \cdot 10^{-6}$ m) in (6) yields a representative friction factor $f_w \approx 0.1$. This estimate is slightly smaller than the friction factors inferred by *Young and Gorman* [1995] from the attenuation of energetic swell observed on the southern coast of Australia (cf. the $C_f \equiv f_w/2$ estimates given by *Young and Gorman* [1995, Figure 16]).

The friction factors suggested by both *Young and Gorman*'s [1995] study and the present observations are much larger than those commonly used in wave prediction models [e.g., *The WAMDI Group*, 1988]. The inferred large friction factors are believed to occur only on very rough (e.g., rippled) bottoms. *Tolman* [1994] presented a simple model for wave-generated bed forms and the associated damping of swell across a continental shelf based on a wave bottom boundary layer model by *Madsen et al.* [1988] and a movable bed roughness model by *Grant and Madsen* [1982]. Tolman's simulations suggest that moderately energetic swell shoaling on a continental shelf can generate sand ripples that greatly enhance the bottom roughness and result in strong damping of the swell. The conditions for the sudden onset of ripple formation (when the near-bed orbital flow exceeds the threshold for sediment motion) in Tolman's simulations are very similar to the midshelf depth and wave conditions of Figure 6. Thus a possible explanation for the observed attenuation of swell is rough bed forms generated by the waves. Unfortunately, no information on the seabed roughness is available to test this hypothesis. Simultaneous measurements of swell attenuation and bottom roughness are needed to determine the possible importance of wave-generated and other bed forms in the evolution of swell across continental shelves.

6. Summary

The transformation of swell across a wide, irregular continental shelf was examined with data collected offshore of Duck, North Carolina. A 100 km long cross-shelf transect of 10 bottom pressure recorders, extending from near the shore (6 m depth) to the shelf break (87 m depth), was deployed for a 4 month long period spanning a wide range of conditions. The present analysis is restricted to periods of light local winds when surface boundary layer processes (e.g., wave generation by wind and wave breaking in the form of whitecaps) are relatively unimportant and the transformation of swell across the shelf is expected to be dominated by bottom effects (e.g., shoaling, refraction, and bottom friction). The selected data records generally show weak variations in swell energy levels across the shelf during benign conditions, but a strong monotonic swell decay between the shelf break and the shore was observed when incident swell energy levels were maximum.

The effects of the irregular shelf bathymetry on the propagation of swell were investigated through simulations with a spectral refraction model for a range of incident wave conditions. Although the ray trajectories are sensitive to the multiple, ridge-like bathymetric features on the shelf, the predicted energy variations for realistic swell spectra are weak. Predictions of the energy-conserving refraction model agree reasonably well with the weak variation in swell energy levels observed across the shelf during benign conditions. Although the model-data comparisons are somewhat qualitative because accurate measurements of the directional properties of incident waves were not available, the results indicate that small-amplitude swell is not significantly dissipated on the shelf.

The observed attenuation of high-energy swell across the shelf is not predicted by the refraction model. The large discrepancy (up to a factor 4) between predicted and observed energy levels near the shore suggests that energetic swell is strongly attenuated by bottom boundary layer processes on the continental shelf.

Acknowledgments. This research was supported by the Office of Naval Research Coastal Dynamics Program. The pressure recorders were designed and built by principal engineer Mike Kirk and deployed by the staff of the Scripps Institution of Oceanography Center for Coastal Studies and the Naval Postgraduate School Department of Oceanography. We thank Paul Jessen for analyzing and archiving the measurements, Captain Dick Ogus and the crew of the R/V *Cape Hatteras* for excellent support during mooring deployment cruises, and Steve Elgar for his help with the recovery of instruments. Helpful discussions with Bob Guza, John Trowbridge, and Hendrik Tolman are also much appreciated.

References

Berkhoff, J. C. W., Computation of combined refraction-diffraction, paper presented at 13th International Conference on Coastal Engineering, Am. Soc. of Civ. Eng. Vancouver, B. C., Canada, 1972.

Graber, H. C., M. W. Byman, and W. Rosenthal, Numerical simulations of surface wave refraction in the North Sea, part 1, Kinematics, *Dtsch. Hydrogr. Z.*, *43*, 1–18, 1990.

Grant, W. D., and O. S. Madsen, Movable bed roughness in unsteady oscillatory flow, *J. Geophys. Res.*, *87*, 469–481, 1982.

Grant, W. D., and O. S. Madsen, The continental shelf boundary layer, *Annu. Rev. Fluid Mech.*, *18*, 265–305, 1986.

Hasselmann, K., et al., Measurements of wind wave growth and swell decay during the Joint North Sea Wave Project (JONSWAP), *Dtsch. Hydrogr. Z.*, *A8*, suppl., 95 pp., 1973.

Haus, B. K., H. C. Graber, L. K. Shay, and J. Martinez, Ocean surface current observations with HF Doppler radar during the DUCK94 experiment, *Tech. Rep. RSMAS 95-010*, 39 pp., Univ. of Miami, Miami, Fla., 1995.

Hwang, P. A., E. J. Walsh, W. B. Krabill, R. N. Swift, S. S. Manizade, J. F. Scott, and M. D. Earle, Airborne remote sensing applications to coastal wave research, *J. Geophys. Res.*, *103*, 18,791–18,800, 1998.

Kirby, J. T., A general wave equation for waves over rippled beds, *J. Fluid Mech.*, *162*, 171–186, 1986a.

Kirby, J. T., Higher-order approximations in the parabolic equation method for water waves, *J. Geophys. Res.*, *91*, 933–952, 1986b.

Kirby, J. T., Open boundary condition in the parabolic equation method, *J. Waterw. Port Coastal Ocean Eng.*, *112*, 460–465, 1986c.

Le Méhauté, B., and J. D. Wang, Wave spectrum changes on a sloped beach, *J. Waterw. Port Coastal Ocean Eng.*, *108*, 33–47, 1982.

Long, R. B., Scattering of surface waves by an irregular bottom, *J. Geophys. Res.*, *78*, 7861–7870, 1973.

Longuet-Higgins, M. S., On the transformation of a continuous spectrum by refraction, *Proc. Cambridge Philos. Soc.*, *53*, 226–229, 1957.

Lygre, A., and H. E. Krogstad, Maximum entropy estimation of the directional distribution in ocean wave spectra, *J. Phys. Oceanogr.*, *16*, 2052–2060, 1986.

Madsen, O. S., Y.-K. Poon, and H. C. Graber, Spectral wave attenuation by bottom friction: Theory, paper presented at 21st International Conference on Coastal Engineering, Am. Soc. of Civ. Eng., Malaga, Spain, 1988.

Munk, W. H., and R. S. Arthur, Wave intensity along a refracted ray, in *Gravity Waves*, *Circ. 521*, pp. 95–108, Natl. Bur. of Stand., 1951.

Munk, W., and M. Traylor, Refraction of ocean waves: A process linking underwater topography to beach erosion, *J. Geol.*, *1*, 1–26, 1947.

O'Reilly, W. C., and R. T. Guza, Comparison of spectral refraction and refraction-diffraction wave models, *J. Waterw. Port Coastal Ocean Eng.*, *117*, 199–215, 1991.

O'Reilly, W. C., and R. T. Guza, A comparison of two spectral wave models in the Southern California Bight, *Coastal Eng.*, *19*, 263–282, 1993.

O'Reilly, W. C., R. J. Seymour, R. T. Guza, and D. Castel, Wave monitoring in the Southern California Bight, paper presented at 2nd International Symposium on Ocean Wave Measurement and Analysis, New Orleans, La., Am. Soc. of Civ. Eng., July 25–28, 1993.

Panchang, V. G., G. Wei, B. R. Pierce, and M. J. Briggs, Numerical simulation of irregular wave propagation over a shoal, *J. Waterw. Port Coastal Ocean Eng.*, *116*, 324–340, 1990.

Porter, D., and D. J. Staziker, Extensions of the mild-slope equation, *J. Fluid Mech.*, *300*, 367–382, 1995.

Putman, J. A., and J. W. Johnson, The dissipation of wave energy by bottom friction, *Eos Trans. AGU*, *30*, 67–74, 1949.

Radder, A. C., On the parabolic equation method for water-wave propagation, *J. Fluid Mech.*, *95*, 159–176, 1979.

Shemdin, O. H., V. Hsiao, H. E. Carlson, K. Hasselmann, and K. Schulze, Mechanisms of wave transformation in finite water depth, *J. Geophys. Res.*, *85*, 5012–5018, 1980.

Snodgrass, F. E., G. W. Groves, K. F. Hasselmann, G. R. Miller, W. H. Munk, and W. H. Powers, Propagation of ocean swell across the pacific, *Philos. Trans. R. Soc. London*, *Ser. A*, *259*, 431–497, 1966.

The WAMDI Group, The WAM model—A third generation ocean wave prediction model, *J. Phys. Oceanogr.*, *18*, 1775–1810, 1988.

Tolman, H. L., An evaluation of expressions for wave energy dissipation due to bottom friction in the presence of currents, *Coastal Eng.*, *16*, 165–179, 1992.

Tolman, H. L., Wind waves and movable-bed bottom friction, *J. Phys. Oceanogr.*, *24*, 994–1009, 1994.

Watson, D. F., ACORD: Automatic contouring of raw data, *Comput. Geosci.*, *8*, 97–101, 1982.

Young, I. R., and R. M. Gorman, Measurements of the evolution of ocean wave spectra due to bottom friction, *J. Geophys. Res.*, *100*, 10,987–11,004, 1995.

E. J. Hendrickson and T. H. C. Herbers, Department of Oceanography, Naval Postgraduate School, Monterey, CA 93943-5122. (herbers@oc.nps.navy.mil)

W. C. O'Reilly, Center for Coastal Studies, Scripps Institution of Oceanography, La Jolla, CA 92093-0209.

(Received May 24, 1999; revised March 21, 2000; accepted March 31, 2000.)